

Application of Remote Sensing and Geographic Information Systems to Forest Fire Hazard Mapping

Emilio Chuvieco

Department of Geography, University of Alcala de Henares, Madrid, Spain

Russell G. Congalton

Department of Forestry and Resource Management, University of California, Berkeley

Digitally processed Thematic Mapper data were integrated with other layers of geographic information to derive a forest fire hazard map. The test area was located in the mediterranean coast of Spain, which is one of the countries most affected by forest fires in Europe. The area suffered a severe forest fire in 1985. Therefore, comparison between the predicted hazard and the actual burned area was possible. More than 22% of pixels with high hazard values in the whole study area were burned by the fire, while only 3.74% of those with low hazard values were actually burned.

INTRODUCTION

In recent years, the effects of natural or man-caused catastrophes have emphasized the need for developing a broader view of many natural processes. The "global monitoring" approach (Goward et al., 1987) tends to consider environmental problems

from this perspective, and favors the understanding of the complexity underlying natural phenomena.

It is quite obvious that this global approach requires the use of new techniques for obtaining, processing, and displaying spatial information in a timely and cost-effective way. This is the main objective of the Geographic Information System (GIS) approach. A GIS takes advantage of a computer's abilities to store and process great volumes of data (Burrough, 1987). Therefore, it makes it possible to update or retrieve spatial information, as well as to derive cartographic models by combining, in different ways, the layers of information included in the data base.

Forest fire research is one of many appropriate GIS applications. The diversity of factors that affect the beginning and spreading of a forest fire dictates the use of an integrated analysis approach. Considering the intrinsic dynamism of this phenomenon, remote sensing imagery is also very valuable for these kinds of studies. It provides a quick evaluation of the vegetation status, as well as a survey of the effects of fire upon the environment. This paper deals with the application of both GIS and remote sensing techniques for fire

Address correspondence to Dr. Russell G. Congalton, Dept. of Forestry and Resource Mgmt., 145 Mulford Hall, Univ. of California, Berkeley, CA 94720.

Received 22 November 1988; revised 9 June 1989.

hazard mapping. The study is centered upon the mediterranean coast of Spain, one of the most affected areas by forest fires in Europe. It should be noted that this study deals with fire hazard which can be defined as a measure of the fuel sources available for burning. Fire risk models include ignition sources such as lightning as well as fuel sources.

FIRE HAZARD MODELS FROM REMOTE SENSING

Different remote sensing techniques have been widely employed for forest fire mapping and prevention. The first applications of remote sensing to forest fire mapping date from the 1960s when several aerial infrared scanners were tested for fire spot detection. A bispectral sensor (middle and thermal infrared) became operational in 1970 for fire source detection in Montana and Idaho (Hirsch et al., 1971).

With the development of the Landsat program, several projects were conducted to test the reliability of satellite imagery for forest fire mapping and inventory (Chuvieco and Congalton, 1988b). Although several sources of confusion between burned vegetation and other land cover types were found (Benson and Briggs, 1978; Tanaka et al., 1983; Husson, 1982), the effectiveness of this approach has proven very useful for a quick evaluation of the damaged area (Isaacson et al., 1982; Arbiol et al., 1987).

In addition to forest fire mapping and inventory, remote sensing has also been effectively used for fire hazard mapping. The use of a GIS approach has made it possible to combine several variables in order to establish fire hazard areas. The main factors included in these models were vegetation, relief (elevation, slope, and aspect), insolation, fire history, and weather data, which are the critical factors in any fire hazard rating system (Deeming et al., 1978; Calabri, 1984; Artsybashev, 1983).

In these studies, digital processing of Landsat MSS images was employed to obtain fuel-oriented vegetation maps. Several authors reported a significant correlation between digital classifications and downed fuel classes obtained by field work (Rabii, 1979). Other studies attempted to derive National Fire Danger Rating System (NFDRS) fuel types

from MSS images. Digital elevation data were frequently used in these studies to improve the discrimination of some fuel classes (Shasby et al., 1981). The results were quite satisfactory and, therefore, these fuel types were effectively used for computing the NFDRS energy release component or for predicting fire behavior (Burgan and Shasby, 1984; Agee and Pickford, 1985; Root et al., 1986). Other authors were less confident about the application of space-borne sensors to fuel mapping. The main reason for this doubt involves the difficulties in discriminating the understory component of the forest vegetation (Salazar, 1982).

A more integrated approach for fire hazard mapping was developed for the FIREScope project. Vegetation (from Landsat imagery) was geo-referenced along with slope, elevation, aspect, soils, insolation, water availability, and fire history, to produce very interesting models (Cosentino et al., 1981; Yool et al., 1985). Similar approaches, on a more limited scale, have been taken by other authors (Brass et al., 1983).

In recent years, several projects have demonstrated the use of AVHRR images for forest fire research. Several studies have been conducted both for fire detection (Matson et al., 1984; Muirhead and Cracknell, 1985; Flannigan and Vonder Haar, 1986; Matson and Holben, 1987) and for fuel mapping (Miller and Johnston, 1985; McKinley et al., 1985; Werth et al., 1985). The increased frequency of data acquisition, as well as the cost-accuracy relationship, make it a good alternative to Landsat, especially when information is required over large areas. A combined analysis of AVHRR and aerial scanner data has proven very useful for the study of critical variables of a forest fire in near-real time (Ambrosia and Brass, 1988).

OBJECTIVES

The objective of this project was to establish a reliable method for fire hazard mapping in a mediterranean environment. Two original aspects were incorporated into this study. First, the use of high resolution imagery (i.e., Landsat TM), which is assumed to render a significant improvement in the fuel-oriented vegetation mapping. Second, the choice of a test area that was already affected by forest fire. Choosing an area that has had a fire makes it possible to assess the reliability of the

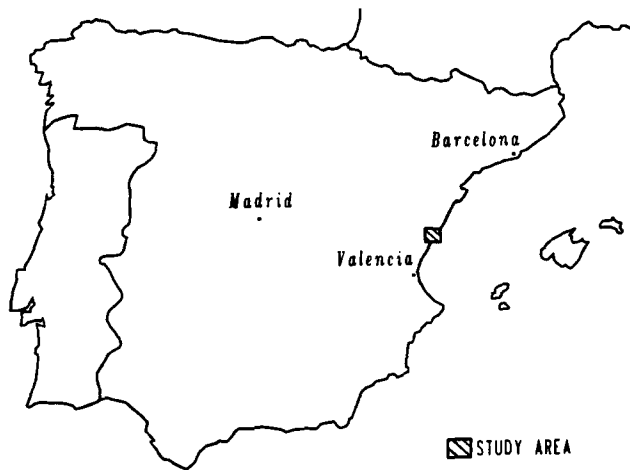


Figure 1. Location map.

hazard mapping. In other words, it can be tested whether the predicted high-hazard areas matched the actual area affected by the fire.

METHODS

Geographical Characteristics of the Test Area

The test area is located in the mediterranean coast of Spain, a few miles north of the city of Castellón (Fig. 1). The area under study was disturbed by an important forest fire in August 1985. It extensively scorched one of the most important ecological and recreational areas in the region. The fire was started by undetermined causes and was quickly spread by the local winds.

The area has the typical characteristics of a mediterranean environment, and therefore it is ranked as a high-hazard area for forest fires. The primary vegetation is composed of conifers, mainly Aleppo pine (*Pinus halepensis*), and a variety shrub species. Both cover types are composed mostly of xerophytic plants, which have resistant leaves and/or high resin or essential oil content, and therefore are highly flammable. The relative humidity of the area is typically very low during July and August, while the strong on-shore winds increase the evapotranspiration rate and aid the spread of the fire once it starts.

The topography of the area is complex due to the presence of several coastal ranges (Sierra del Desierto de las Palmas and Montes de Villafams). The slopes tend to be medium or steep, which notably complicates the digital image classification

(Chuvieco and Congalton, 1988a). Only in the vicinity of the shoreline has a littoral plain developed, which is used for agricultural production, mainly citrus trees and orchards.

The agricultural, as well as the natural land cover, shows an extreme fragmentation in the area analyzed. The traditional cultural practices in this zone have lead to a very complex parcel structure. Many of the agricultural properties, especially the irrigated crops, are less than 1 ha in size. This fragmentation complicates the classification task by introducing many pixels with a mixed signature as a result of the boundary effect. In the forest land the problem is also important, although in this case it is caused by a frequent mixture between forest and scrub with various densities and stand heights.

An Integrated Approach

As previously stated, the main purpose of this project was to obtain a reliable fire hazard map of the study area. The variables in the model included the basic factors that affect forest fires in the mediterranean environment:

1. vegetation species, classified according to fuel class, stand conditions, and site,
- b. elevation,
- c. slope,
- d. aspect,
- e. proximity to roads and trails, campsites, or housing.

Each one of these variables was considered as a different layer of information for the integrated analysis. The overlaying of all these variables made it possible to define fire hazard levels within the study area. Then, those areas with the highest hazard were compared with the actual area disturbed by the fire. The burned land was discriminated using a Thematic Mapper image acquired a few hours after the fire. The agreement between the predicted high-hazard areas and the actual burned land was assumed to be a major test about the reliability of the study approach.

Vegetation Mapping

The main factor affecting the spread of a forest fire is the type and characteristics of the vegetation. Both overstory and understory are crucial because

they represent the total fuel available for the fire. Traditional Landsat classification tends to derive land cover maps, which divide the vegetation into homogeneous areas of different species (e.g. pine trees, oak trees, manzanita, etc.) or into zones of different associations (e.g., conifer stands, chaparral, shrub, etc.). From a forest fire perspective, it would be optimum to not only know vegetation species but also to be able to discriminate different stand densities, height–area ratios, and stress conditions. This approach has not been reliable from Landsat MSS imagery because of the spectral and spatial resolution limitations. Information about the understory has not been reliable either. In this project, the vegetation mapping was improved by using TM instead of MSS images. This improvement can be attributed better discrimination of forest density and structure as well as increased detection of the understory (Stenback, 1988).

The image selected for processing was acquired on 26 June 1984. This image presented good cloud-free coverage as well as convenient phenological conditions for discriminating different vegetation species. The objective of the digital classification was to produce a detailed map of the vegetation types and characteristics of the study area. Using visual analysis, nonvegetation covers like water and urban land were dropped from the analysis using a spatial masking technique. This spatial masking made it possible to avoid some of the typical confusion in digital classification between vegetation and nonvegetation categories. Masking of nonvegetation classes was performed by digitizing and cutting out on the screen the chosen areas (Fig. 2). Cultivated fields were retained because of their great spatial diversity. These fields can be a major cause of forest fires because the burning of straw is still used to produce fertilizer in some parcels.

Standard supervised classification techniques were applied to the TM imagery. Aerial photography acquired in 1985 by the Spanish National Geographic Institute was available for the selection of training fields. The timelag between the TM image and the aerial photography (1 year) was not a severe problem in using it for this purpose. Several fields were located for each of the vegetation species, according to different densities, volume, and topographic position. Unsupervised analysis was used to supplement the process and made

it possible to obtain a better statistical definition of some of the classes. A complete description of this process can be found in Chuvieco and Congalton (1988a). A total set of 16 categories were generated using a maximum-likelihood classifier. Four categories of pine trees and six of shrub species were distinguished, according to density, aspect, and site characteristics.

Topographic Data

Topography is one of the main factors included in any fire hazard rating system. The impacts of elevation, aspect, and slope in fire behavior have been widely reported in the literature (Brown and Davis, 1973; Artsybashev, 1983). Among them, slope is considered the critical factor. Steep slopes increase the rate of spread because of a more efficient convective preheating and ignition by point contact. Slope also has a major effect in the suppression of the fire, because it affects crew fatigue, rolling material, and safety. It has been reported that vegetation on smooth, broad slopes tends to burn more completely than on slopes containing watercourses or cliffs, which interrupt the forward movement of fire (Minnich, 1978). Aspect and exposure are very much related to the rate of fuel drying and spread of the fire. Lastly, higher elevations are related to greater rain availability. Therefore, the fires tend to be less severe at higher elevations. However, in the study area, the elevation range (800 m) does not involve a great rainfall difference between the highest and the lowest areas.

Slope, aspect, and elevation are usually obtained from digital terrain models. In the case of Spain, these data are not yet available. Therefore, an elevation model for the study area was created from 1:50,000 topographic maps. Main contours were digitized and the point coordinates input into a grid conversion program. A set of 8765 points was employed for the point to grid conversion process. Average weighing by the inverse distance (at the fourth power) was employed as the interpolation method. The calculations were made considering the four nearest points to each cell, one per quadrant. Slope and aspect were computed from the elevation data. The slope image was graduated into 4% intervals, while aspect was divided into 2° intervals.

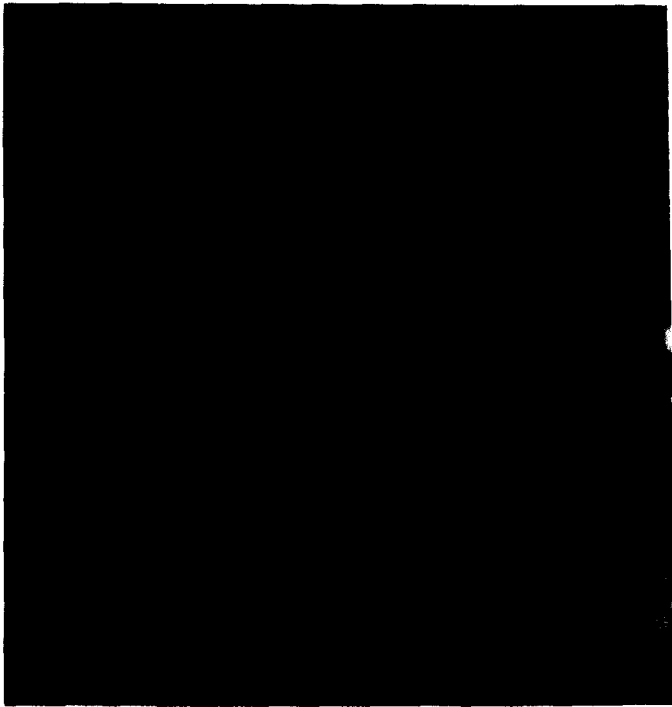


Figure 2. False color composite of the Thematic Mapper image of the study area. Urban land and water were masked out to improve the discrimination of the vegetation categories. The area affected by the fire is outlined in white.

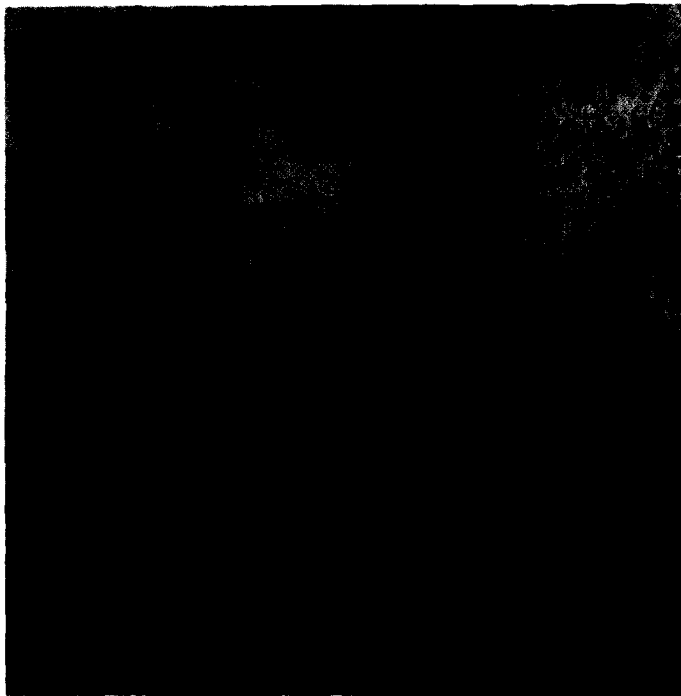


Figure 3. Vegetation map. Green tones indicate different types of pine trees; brown, orange, and magenta, different types of shrub; and yellow and blue tones represent agricultural land.

Proximity Analysis

Trail and road locations are also an important factor in fire hazard mapping. Two major effects can be considered. First, they can serve as fire breaks or pathways for suppression of the fire. In this sense, they are a reducing factor of fire hazard. Second, they are potential routes for hiking or camping areas. In this context, they increase forest fire hazard because of the more intense human activity.

In spite of the obvious importance of roads and trails, this information has not commonly been used in fire hazard models. The difficulties in dealing with linear features in any raster data structure may be one reason why these data are usually missing. New techniques for combining vector and raster structures make it possible to achieve the desired integration.

In this project, roads and trails were digitized and analyzed using PC ARC/INFO. A buffer distance of 50 m was established for the main roads (which are made of concrete or asphalt), while a distance of 150 m was selected for trails and fire breaks. A longer distance was selected for trails because it was assumed that the human impacts on these paths are more diffuse. In other words, the impact is not as confined as in the roads. These buffered zones were assumed to be the most likely areas for fire starting with respect to roads and trails. The buffered map was rasterized and registered with the other layers of information to derive the final fire hazard map.

Fire Hazard Modeling

Any GIS is only a tool for storage, analysis, and display of spatial data. It is very helpful to maintain a coherent and common structure for the data, but it does not provide any cartographic model by itself. In other words, use of GIS presupposes the presence of a previous theory which makes it possible to combine the variables in a meaningful and efficient way.

Most of the studies on fire hazard mapping have not dealt with fire hazard modeling. Typically, they derived fuel classes from satellite imagery and topographic data to be input in a standard fire hazard rating system. (Burgan and Shasby, 1984; Root et al., 1986; Agee and Pickford, 1985).

Other projects have focused on obtaining the source variables (vegetation, topography, insolation, and fire history), but they have not attempted to integrate the variables into a single fire hazard index (Cosentino et al., 1981; Yool et al., 1985). One of the few studies based only on spatial layers was developed by Brass et al. (1983). In this case, a qualitative model (low, moderate, high, and very high fire hazard) from vegetation and slope characteristics was proposed.

In our study, the intent was to integrate the spatial data layers in a single fire hazard index, which could be used for mapping later on. Five layers of information were available: vegetation, slope, aspect, elevation, and proximity to roads. The integration of these variables was adopted in a

Table 1. Fire Hazard Modeling Method

Original Classes	Fire Hazard Groups	Coefficient
<i>1.1. Vegetation Layer (Weight 100)</i>		
Dense pine tree	high	0
Medium pine tree	high	0
Sparse pine tree + shrub	medium	1
Dense shrub	medium	1
Medium shrub	medium	1
Sparse shrub	low	2
Almond trees	low	2
Vineyards	low	2
Orange trees	low	2
<i>2.1. Slope Layer (Weight 30)</i>		
0–4%	low	2
5–8%	low	2
9–12%	low	2
13–16%	medium	1
17–20%	medium	1
21–36%	medium	1
27–40%	medium	1
41–44%	high	0
> 44%	high	0
<i>2.3. Aspect Layer (Weight 10)</i>		
Southeast	high	0
Southwest	medium	1
North	low	2
<i>2.4. Proximity to Roads Layer (Weight 5)</i>		
Inside buffered area (< 150 m from any trail or < 50 m from any road)	high	0
Outside buffered area	low	1
<i>2.5. Elevation Layer (Weight 2)</i>		
0–3 m	low	1
3–6 m	low	1
398–400 m	high	0
401–404 m	high	0
405–407 m	high	0

hierarchical scheme. In other words, it was assumed that some layers have a higher influence on fire hazard than others. According to the literature and to the environmental characteristics of the study area, they were ranked in the following order: vegetation, slope, aspect, proximity to roads, and elevation.

The approach adopted to develop the fire hazard map followed several steps (Table 1). First, each data layer was weighted according to its impact on increasing the fire hazard. Weights were selected in order to scale the final map between 0 and 255. Although it is an arbitrary weighing system, these weights tend to take into account the relative importance of each variable (layer) as a factor for increasing the fire hazard. Second, each data layer was then divided into different levels which were assigned a coefficient of 0, 1, and 2 based on a ranking of high, medium, and low fire hazard, respectively. In those data layers divided

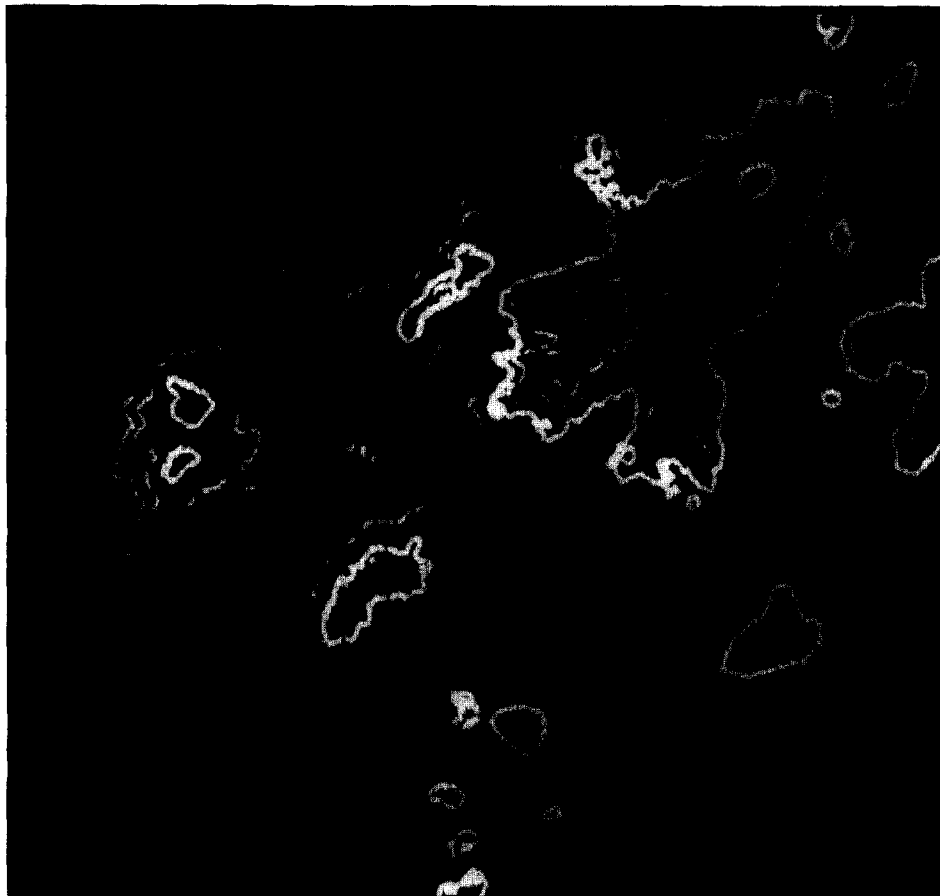
into only two levels, 0 and 1 were assigned to high and low hazard, respectively. Therefore, the lower the hazard index, the higher the hazard of forest fire in that area.

In summary the final formula of the hazard index can be expressed as:

$$H = 1 + 100v + 30s + 10a + 5r + 2e,$$

where v , s , a , r , and e are the coefficients applied to the vegetation, slope, aspect, roads, and elevation groups, respectively. A hazard index of zero was reserved for water and urban land which were dropped from the model. For this reason, 1 is a constant added to the equation to avoid pixels having zero values. Values higher than 255 were reduced to 255 for maintaining the output image in a 8-bit range. This decision does not involve an important loss in data, because it corresponds to the values with a low forest fire hazard.

Figure 4. Slope groups for the fire hazard model. White indicates areas above 40% slope (high hazard); medium grey, between 12 and 40% (medium hazard), and dark grey, below 12% (low hazard).



The groups within each one of the data layers were formed according to a literature review and field experience obtained from the study area. Table 1 gives a complete account of the process. For instance, the vegetation layer was divided in three groups: 1) high and medium dense pine trees; 2) dense and medium shrub; and 3) sparse shrub and agricultural categories. The coefficients for these groups were 0, 1, and 2, respectively. Considering that the vegetation layer had a weight of 100, this meant that vegetation type has the main role in ranking the hazard index values. Final hazard values of 1, 101, or 201 were assigned to all the pixels having a vegetation type of 1), 2), or 3), respectively [e.g., $H = 1 + 100(1) = 101$].

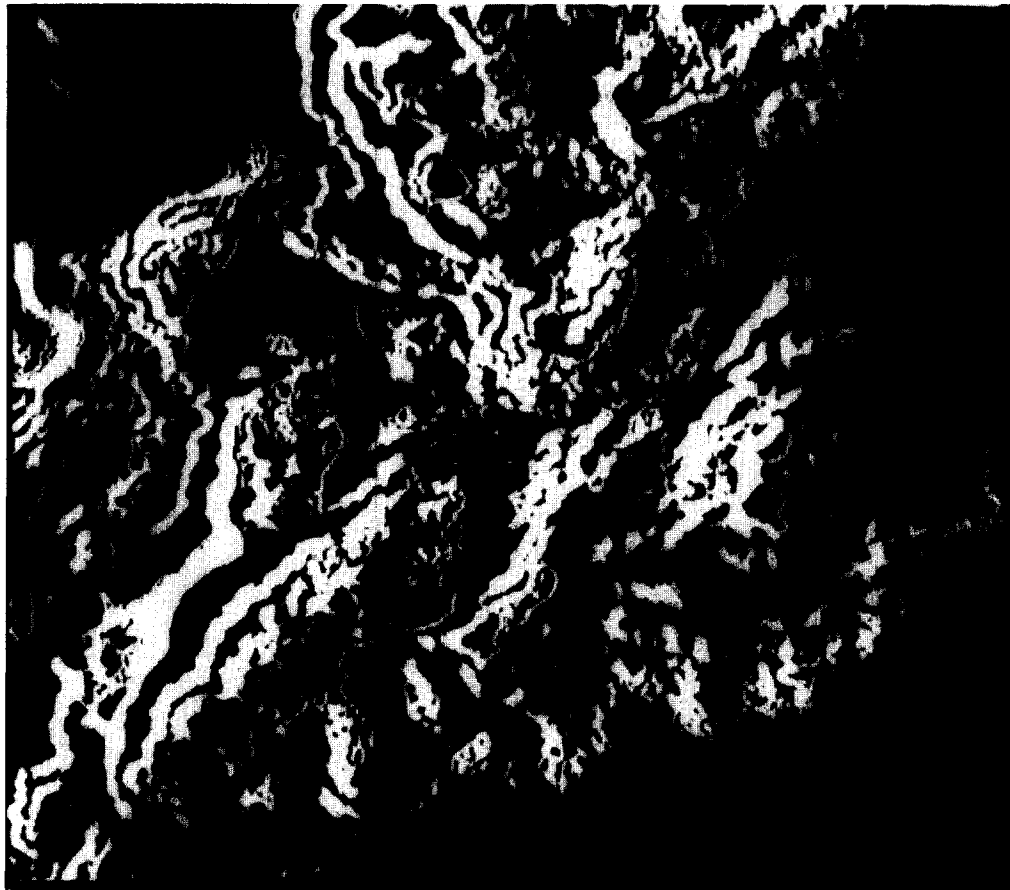
The slope layer was divided in three groups: over 40% (high hazard), between 12 and 40% (medium hazard), and under 12% (low hazard). These thresholds were established in the data because they represent notable changes in the histogram of the slope image. In addition, 40% has been often reported as a crucial threshold for fire

operations (Brass et al., 1983). Similarly to the vegetation, coefficients of 0, 1, and 2 were assigned to these groups. Again, the lower coefficients indicate the higher fire hazard. These coefficients are multiplied by the weighing factor of slope (30) and added to the value previously obtained from the vegetation layer.

Aspect was divided in three groups: southeast (90–180°), southwest (180–270°), and north (270–90°). Southeast slopes present a higher fire hazard because of the higher insolation in this area as well as because it corresponds to the main direction of the local winds. Again, coefficients associated with these groups were 0, 1, 2, and aspect value was added to the one obtained from vegetation and slope.

The proximity to roads layer was divided in two groups: inside and outside the buffered area. The inside corresponds to all pixels within a radius of 150 m from any trail or of 50 m from any road. This area was considered to have the higher fire hazard and, therefore, it was assigned a coefficient

Figure 5. Aspect groups for the fire hazard model. Dark grey, southeast (high hazard); medium grey, southwest (medium hazard); and white, north (low hazard).



of 0. Pixels outside this zone were assigned a coefficient of 1. Values were added to the ones obtained from previous layers.

Finally, the elevation layer was divided in two groups as well. The boundary was established at 400 m of elevation. This value tends to separate the local Sierras from the plains. Coefficients of 0 (high altitudes, high hazard) and 1 (lowlands) were applied. Again, the values are summed to the previous layers.

A FORTRAN program was written to perform these calculations and to output an 8-bit binary image. This image could then be overlaid on a burned land map obtained from a Thematic Mapper image acquired after the fire. In doing so, it was possible to compute the hazard-index values of the pixels that were actually burned. In other words, the effectiveness of this method of fire hazard mapping was tested by comparisons with the area actually affected by the fire.

RESULTS

Obtaining the Information Layers

Figures 3–7 present the five layers of information that were developed for this study. Vegetation was obtained from a combined supervised and unsupervised classification of a TM image acquired on 26 June 1984. Sixteen categories were discriminated. These included different species as well as site and stand conditions. No extensive, quantitative accuracy assessment was performed on this classification. However, familiarity with the study site and assessments made from previous work in the area (Chuvieco and Congalton, 1988a) confirmed the quality of the results.

The method used for obtaining the elevation data was not as accurate as we had wished. However, it was the best available when the project was performed. The main problem seems to be related to the interpolation algorithm, which does

Figure 6. Proximity to Roads. Light grey indicates the areas within the established buffer distance to any road (50 m) or any trail (150 m).



not conveniently smooth the transitional areas. Slope and aspect were computed from the elevation data.

The proximity to roads data was the most difficult to obtain. In order to preserve the original shape of the roads, the analysis was performed by a vector GIS program. Roads and trails were digitized and stored in different files. Then, a buffer area was computed along each trail and road according to the previous distance settings (150 m for trails; 50 m for roads). The final map was rasterized and overlaid with the other images.

Fire Hazard Mapping

The final hazard-index map is displayed in Fig. 8. Geometric corrections made it possible to overlay this image with the one acquired after the fire. Hazard-index values for pixels within the boundary of the burned area were extracted. Analysis of those values provided an insight about the consistency of our approach. A summary of the results is

presented in Tables 2 and 3. From these data, several comments can be made:

—The area affected by the fire includes a variety of land covers, even agricultural categories. Therefore, the histogram of hazard-index values does not present a clear bias to the low values (high hazard areas). This result is not surprising and means that even areas with a low predicted hazard were actually burned. That should not imply a rejecting of the method, because it only tries to measure the fire hazard not the fire behavior or the fire risk. Fire hazard is more related to the fuel sources, while fire risk includes both fuel and ignition sources and fire behavior is dynamic. Factors not considered here, such as moisture, wind speed, and direction, have a strong influence in the actual area burned by the fire.

—Other factors, besides vegetation, used in the fire hazard model did not predict that an area would be burned as well as might have been expected. For instance, the burned area includes primarily medium or low slopes (under 40%), which

Figure 7. Elevation groups for the fire hazard model. Light grey, areas below 400 m (low hazard); white, areas above 400 m (high hazard).



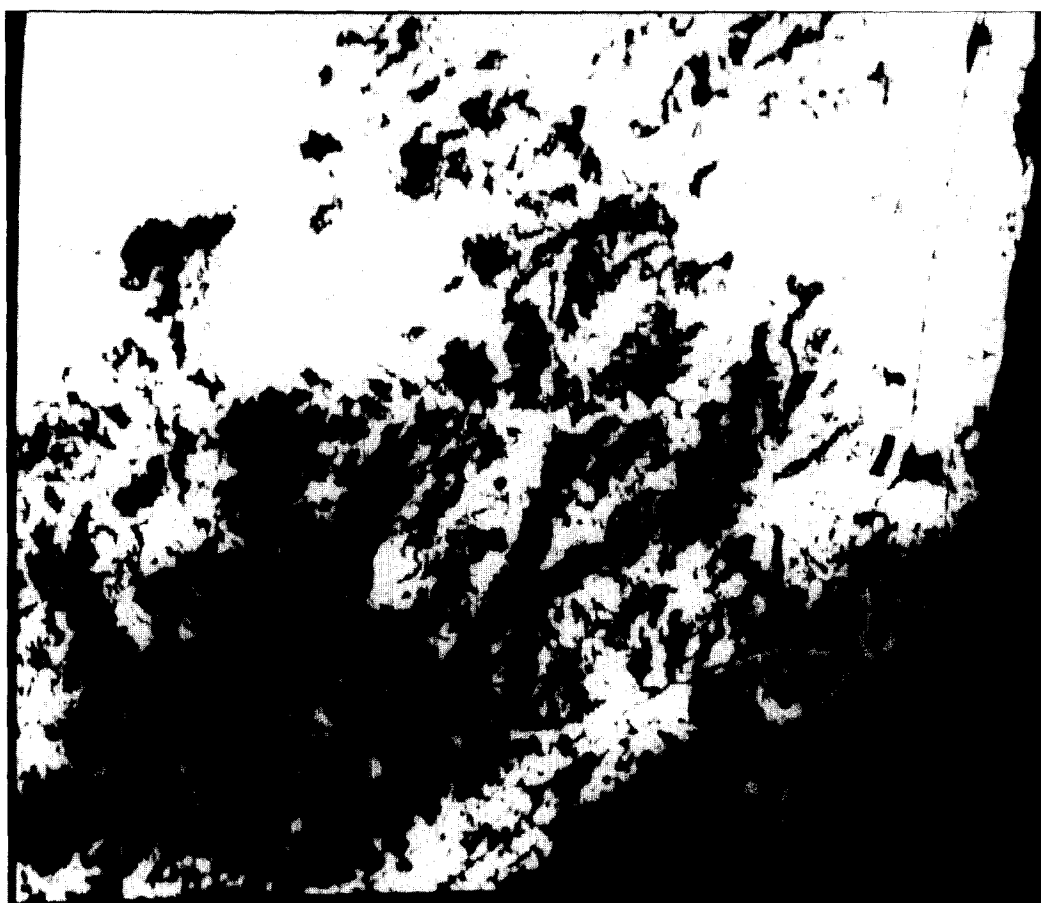


Figure 8. Hazard index map. For display purposes, the whole range of hazard index values has been divided in three categories: 1) high hazard (1–100); 2) medium hazard (101–200); 3) low hazard (201–255).

were ranked as medium and low hazard, respectively. Distribution of proximity to roads and elevation data in the burned area did not seem to agree that well either. Within the burned land, 35.07% was included in the road buffered zone, while only 19.60% had an elevation higher than 400 m. The best results were obtained for the aspect layer. Inside the perimeter of the scorched

zone, 39.51% of the area was on a southeast aspect, 24.07% on a southwest aspect and 35.55% on a north aspect.

From the discussion above, it could be viewed that our model performed poorly in predicting the burned area. However, it should be stated again than the model tried to predict fire hazard and not fire behavior. Therefore, the question is not whether all the burned land had a high hazard of being burned, but rather to find out the proportion of the high hazard areas that were actually burned by the fire. From this perspective, the model can be considered as more reliable (Table 3). Of the 28,906 pixels classified in the whole study area as high hazard, 6569 were actually burned (22.72%). In the case of low hazard pixels, only 3.74% was actually burned. In other words, high hazard pixels were six times more affected by the fire than low hazard pixels. Therefore, it can be concluded that the model provided valuable information about the most likely areas to be affected by the fire. Further

Table 2. Fire Hazard Index of the Pixels That Were Actually Affected by the Fire^a

Hazard Value	Number of Pixels	%
1–30	629	2.70
31–60	1767	7.59
61–90	4173	17.93
101–130	1022	4.39
131–160	2680	11.52
161–190	8502	36.53
201–230	320	1.37
231–255	4072	17.50

^a Values close to 1 indicate high hazard, while the ones close to 255 indicate low hazard.

Table 3. Proportion of Fire Hazard Values Affected by the Fire in the Study Area

Fire Hazard Value	No. of Pixels inside the Burned Area (a)	No. of Pixels outside the Burned Area (b)	a / b (%)
High hazard value (1–100)	6569	28,906	22.72
Medium hazard value (101–200)	12,204	79,825	15.28
Low hazard value (201–255)	4392	117,509	3.74

research in the selection and grouping of variables should improve the reliability of these predictions.

CONCLUSIONS

An integrated analysis of spatial variables is very valuable for forest fire research. Remote sensing provides a source of vegetation data, while GIS processing made it possible to create fire hazard models. The variables chosen for the study are widely recognized as crucial in forest fire prevention and suppression. The proposed model performed properly in identifying the areas subjected to a higher fire hazard. Comparison with the area actually affected by the fire gives many insights about the validity of the selected variables and about the hazard groups distinguished within them. Further research should be devoted to testing the impacts of selecting new variables (i.e., data layers), or to establishing new boundaries between fire hazard groups within these variables.

This research was performed while Dr. Chuvieco was a Fulbright Scholar at the Department of Forestry and Resource Management of U.C., Berkeley. The authors wish to thank the Spanish Ministry of Education and the Regional Government of Madrid for their funding support. Contributions of Cathy Travlos, Lucy Salazar, Robert E. Martin, and Brad Gallup were notably helpful.

REFERENCES

- Agee, J. K., and Pickford, S. G. (1985), Vegetation and fuel mapping of North Cascades National Park, Final Report, College of Forest Resources, Seattle.
- Ambrosia, V. G., and Brass, J. A. (1988), Thermal analysis of wildfire effects on global ecosystem cycling, *Geocarto Int.* 3:29–40.
- Arbiol, R., Romeu, J., and Vinas, O. (1987), Detecció i evaluació de les superfícies forestals cremades durant l'any 1984 a Catalunya, mitjan cant techniques de Teledetecció, *Rev. Catalana Geogr.* 2(4):21–46.
- Artsybashev, E. S. (1983), *Forest Fires and Their Control*, Oxonian, New Delhi (1st ed. in Russian, 1974).
- Benson, M. L., and Briggs, I. (1978), Mapping the extent and intensity of major forest fires in Australia using digital analysis of Landsat imagery, in *Proc. of the Int. Symp. on Remote Sensing for Observ. and Inventory of Earth Resources*, pp. 1965–1980.
- Brass, J. A., Likens, W. C., and Thornhill, R. R. (1983), Wildland inventory for Douglas and Carson City Counties, Nevada, using Landsat and digital terrain data, NASA Technical Paper 2137, Washington, DC.
- Brown, A. A., and Davis, K. P. (1973), *Forest Fire: Control and Use*, McGraw-Hill, New York.
- Burgan, R. E., and Shasby, M. B. (1984), Mapping broad-area fire potential from digital fuel, terrain and weather data, *J. Forestry* 82:228–231.
- Burrough, P. A. (1987), *Principles of Geographical Information Systems for Land Resources Assessment*, Clarendon, Oxford.
- Calabri, G. (1984), *La Prevenzione degli Incendi Boschivi. I Problemi e le Tecniche della Difesa*, Edagricole, Bologna.
- Chuvieco, E., and Congalton, R. G. (1988a), Using cluster analysis to improve the selection of training statistics in classifying remotely sensed data, *Photogramm. Eng. Remote Sens.* 54:1275–1281.
- Chuvieco, E., and Congalton, R. G. (1988b), Mapping and inventory of forest fires from digital processing of TM data, *Geocarto Int.* 4:41–53.
- Cosentino, M. J., Woodcock, C. E., and Franklin, J. (1981), Scene analysis for wildland fire-fuel characteristics in a Mediterranean climate, in *Proc. 15th Int. Symp. on Remote Sensing of Environment*, ERIM, Ann Arbor, MI, pp. 635–646.
- Deeming, J. E., Burgan, R. E., and Cohen, J. D. (1978), The National Fire-Danger Rating System, U.S. Department of Agriculture, Forest Service, Ogden.

- Flannigan, M. D., and Vonder Haar, T. H. (1986), Forest fire monitoring using NOAA satellite AVHRR, *Can. J. Forest Res.* 16:975-982.
- Goward, S. N., Dye, D., Kerber, A., and Kalb, V. (1987), Comparison of North and South American Biomes from AVHRR Observations, *Geocarto Int.* 2:27-40.
- Hirsch, S. N., Kruckeberg, R. F., and Madden, F. H. (1971), The bi-spectral forest detection system, in *Proc. 7th Int. Symp. on Remote Sensing of Environment*, ERIM, Ann Arbor, MI, pp. 2253-2259.
- Husson, A. (1982), Exemple d'utilisation de la Teledetection en France: la cartographie des feux de foret, in *Le Systeme SPOT d'Observation de la Terre* (G. Rochon and A. Chabreuil, Eds.), L'AQT/SFPT, Montreal, pp. 15-26.
- Isaacson, D. L., Smith, H. G., and Alexander, C. J. (1982), Erosion hazard reduction in a wildfire damaged area, in *Remote Sensing for Resource Management* (Johannsen and Sanders, Eds.), Soil Conservation Society of America, Ankeny, IA, pp. 179-190.
- Matson, M., and Holben, B. (1987), Satellite detection of tropical burning in Brazil, *Int. J. Remote Sens.* 8(3):509-516.
- Matson, M., Schneider, S. R., Aldridge, B., and Satchwell, B. (1984), Fire detection using the NOAA series satellites, NOAA Technical Report NESDIS, Washington, DC.
- McKinley, R. A., Chine, E. P., and Werth, L. F. (1985), Operational fire fuels mapping with NOAA-AVHRR data, in *Pecora X Symposium*, pp. 295-304.
- Miller, W., and Johnston, D. (1985), Comparison of fire fuel maps produced using MSS and AVHRR data, *Pecora X Symposium*, pp. 305-314.
- Minninch, R. A. (1978), The geography of fire and conifer forest in the Eastern Transverse Ranges, California, Ph.D. dissertation, UCLA.
- Muirhead, K., and Cracknell, A. P. (1985), Straw burning over Great Britain detected by AVHRR, *Int. J. Remote Sens.* 6:827-833.
- Rabii, H. A. (1979), An Investigation of the utility of Landsat-2 MSS data to the fire-danger rating area, and forest fuel analysis within Crater Lake National Park, Oregon, Ph.D. dissertation, Oregon State University.
- Root, R. R., Stitt, S. C. F., Nyquist, M. O., Waggoner, G. S., and Agee, J. K. (1986), Vegetation and fire fuel models mapping of North Cascades National Park, *ACSM-ASPRS Annu. Convention Tech. Pap.* 3:78-85.
- Salazar, L. A. (1982), Remote sensing techniques aid in pre-at-tack planning for fire management, Pacific Southwest Forest and Range Experiment Station, Berkeley.
- Shasby, M. B., Burgan, R. R., and Johnson, R. R. (1981), Broad area forest fuels and topography mapping using digital Landsat and terrain data, in *Proc. 7th Int. Symp. on Machine Processing of Remotely Sensed Data*, pp. 529-537.
- Stenback, J. (1988), An assessment of canopy-understory relationships using remotely sensed data, MS Thesis. University of California, Berkeley (94 pp.).
- Tanaka, S., Kimura, H., and Suga, Y. (1983), Preparation of a 1:25,000 Landsat map for assessment of burnt area on Etajima Island, *Int. J. Remote Sens.* 4(1):17-31.
- Werth, L. F., McKinley, R. A., and Chine, E. P. (1985), The use of wildland fire fuel maps produced with NOAA-AVHRR scanner data, in *Pecora X Symposium*, Fort Collins, CO, pp. 326-331.
- Yool, S. R., Eckhardt, D. W., Estes, J. E., and Cosentino, M. J. (1985), Describing the brushfire hazard in Southern California, *Ann. Assoc. Am. Geogr.* 75:417-430.